International Conference on Renewable Energies and Power Quality **(ICREPQ'17)**
Malaga (Spain), 4th to 6th April, 2017
Renewable Energy and Power Quality Journal (RE&PQJ)
ISSN 2172-038 X, No.15 April 2017

Design, Simulation and Performance of a Four Phases Linear Variable Reluctance Motor

B. B. Miranda[1], J. R. Camacho[1] and A. C. F. Mamede[1]

[1] School of Electrical Engineering
Universidade Federal de Uberlandia (UFU)
Campus Santa Mônica – Av. João Naves de Ávila, 2121. Postcode: 38400-902 – Uberlandia (Brazil)
Phone: +55 34 3239 4734, e-mail: brenobritomiranda@hotmail.com, jrcamacho@ufu.br, anacmamede@ufu.br

Abstract *- The linear variable reluctance motor (LVRM) is a motor used in linear applications converting electromagnetic energy into linear movement and thrust. This paper aims at the analytical design of the machine and its validation through the finite element method. The design of a unilateral LVRM model of longitudinal flux type with passive translation movement is developed through the output power equation of the variable reluctance machine (VRM). The finite element analysis (FEA) is applied in order to check the values of inductance, the normal forces and propulsion. The FEA is also necessary to observe the undulation factor (ripple force), highly present in LVRM's, which produces vibration and acoustic noise. The analysis of the relationship between polar arcs and polar pitches plays an important role in the development of LVRM's output force in the reduction of motor weight and volume. The LVRM model is developed from desired parameters, the maximum length of the stator, maximum speed and mass of the translator; through the design of a variable reluctance rotary motor (VRRM). The VRRM specifications are then converted into its linear equivalent.*

Keywords *– finite elements; FEMM; ripple factor, ripple force; linear machines; variable reluctance motors.*

1. Introduction

Linear machines become more attractive as they are used in applications that require linear motion, in which the load can be directly coupled to the moving part, without the need for mechanical conversion (i.e. rotational to translational movement). In [1], a linear vertical propulsion application for an elevator is presented. In [2], a high-precision position control application is discussed. Moreover, in [3], a double-sided linear machine is developed to be used to drive automatic door. Induction motors and permanent magnet linear synchronous motors offer solutions in various industrial applications, particularly where high dynamic performance is required [4]. The linear motors are obtained from the conventional rotary motor in which the stator and the rotor are linearly extended and cut. Although the principle of operation is exactly the same, there are certain differences in relation to rotary motors such as increased length of the air gap and the stator smaller than the guide rail, causing edge effects [5].

The linear variable reluctance motor (LVRM) has simple constructive characteristics with concentrated coils. In addition, because of the need for DC power supply, the converter has a low number of switching devices [6]. However, LVRM has some disadvantages such as high ripple factor on force, vibration and acoustic noise due to double salient structure [7]. There are two types of LVRMs: transverse and longitudinal flux motors. The flux path in cross-flux configuration occurs in the machine moving part direction of movement. This is of more simple construction, is mechanically robust and has less eddy current losses, since the flux is in the same direction of movement [8]. The movable part or rail and the fixed part (stator) are made up of laminations of steel shaped to form the poles [9]. The coils may be fixed both in the fixed part and the moving part. The project developed in this work has the coils attached to the fixed part, because of this it is called the active part, and the rail is the passive part. This topology is advantageous because the active part is smaller than the rail, drastically reducing the use of copper to manufacture the coils. The variable reluctance machine (VRM) is configured such that pairs of coils are connected in series and excited at the same time. The torque is produced by the tendency of the movable part to align at the position where the inductance of the excited coil is maximized [9]. That is, when the pole of the movable portion completely overlaps the poles of the fixed part. The total misalignment is the position where the pole of the fixed part is aligned exactly with the center of the movable rail slot and the inductance of the excited coil is a minimum. The normal force generated tends to decrease the length of the air gap, which is the upward force experienced by the translator. It is caused by the incremental stored magnetic energy during the incremental displacement perpendicular to the translation.

The design of a LVRM four phases unilateral (single-sided) of the longitudinal flux type with fixed active part and passive moving part is studied in this research through FEMM software (Finite Element Method Magnetics) developed by David Meeker with the help of the LUA language. The advantage of using a four-phase LVRM is that this produces less acoustic noise and lower ripple factor in force when compared to a three phase LVRM. The procedure proposed in [8] uses the design of a variable reluctance rotary motor (VRRM) to convert the specifications of the linear machine in its rotating equivalent. The design of the machine is then developed in the rotational field, which is subsequently transformed into the linear domain and the dimensions are chosen [9].

2. Sizing and Topology of LVRM

Fig. 1 shows the cross section view of the structure of an ordinary four-phase longitudinal flux machine. The LVRM contains an active stator (fixed coils) with 8 poles and a passive translator with 8 sequential poles, corresponding to the 8 poles configuration in the stator and 6 poles in the rotor of the 8/6 VRRM rotating machine. Unlike the structure with passive stator and active translator, there is no reverse flux at the time of phase current switching [8]. For the translator to move to the left, the pairs of coils bb', cc', dd' and aa' should be excited in sequence when the position of the poles enter the inductance growing region.

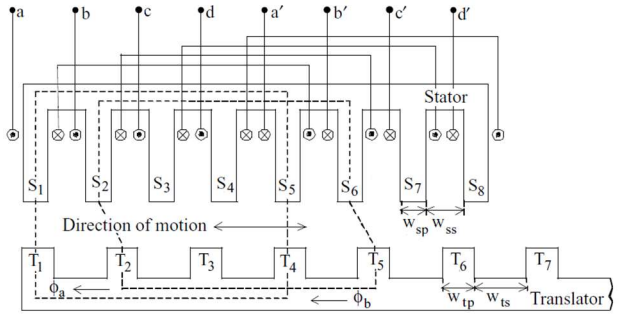

Fig. 1. VRM structure and diagram of windings: the direction of the magnetic flux generated from the excitation of coils of phase a and phase b [8].

A. Output power and parameters of VRM

The model is derived from the output equation for the VRM. This relates the outer diameter of VRRM, length, speed, and the electric and magnetic loading with the machine output power [6]. The output power of the equation is given by

$$P = k_e k_d k_1 k_2 B_g A_{sp} D^2 v_m \frac{60}{\pi} \quad (1)$$

P – output power,
k_e – efficiency,
$k_1 = \pi^2/120$,
k_2 – variable based in the operating point,
k_d – duty cycle,
B_g – flux density at the air gap,
A_{sp} – specific electrical loading,
D – internal diameter,
v_m – maximum speed.

The electromagnetic conversion efficiency k_e is between 0.3 and 0.4. In general, the constant k_2 is chosen from

$$0.65 < k_2 < 0.75 \quad (2)$$

The specific electrical loading is in the following range:

$$25{,}000 < A_{sp} < 90{,}000 \quad (3)$$

The maximum power is developed when k_d =1. The stack width L is given by

$$L = kD \quad (4)$$

where k for general applications is selected from

$$0.25 < k < 0.70 \quad (5)$$

From the dimensions and mechanical characteristics desired – moving part length, maximum speed of the vehicle, acceleration time and maximum load in the translator system - for the LVRM project, the above variables and power capacity, all dimensions of LVRM are calculated [10]. The motor power capacity is given by [8]

$$P = M \frac{v_m^2}{t_a} \quad (6)$$

where

M – mass of the translator system,
v^2_m – maximum speed,
t_a – acceleration time.

Finding the value of P from eq. (6), the variable D is calculated from eq. (1).

1) Minimum polar arcs to start: The right choice of polar arches is critical in maintaining the average torque produced. This is positive in region of growing inductance since the phase current does not enter the region of inductance decline. In order to maintain the starting torque continuous [11], the minimum polar arc in the stator should be chosen by

$$\min(\beta_s) = \frac{4\pi}{P_s P_r} \quad (7)$$

where P_s and P_r are respectively the number of poles of stator and translator in the rotary equivalent. While the translator polar arc must be greater than or at least equal to the stator polar arc:

$$\beta_r \geq \beta_s \quad (8)$$

However, due to the high inductance in the poles aligned region and the complexity in controlling the switching current [8], the rotor polar arc must be greater than the stator polar arc in order to avoid producing negative torque and to improve the driver operational simplicity [8]. But not so greater that the increase on volume of magnetic material increase without feasible gain. Fig. 2 shows the torque generation when the rotor polar arc is greater than the stator polar arc. In this case, any negative output torque doesn´t exist. Other advantages arise when the rated current is kept constant throughout the growth inductance region, increasing the average torque produced when compared to the case in which the polar arcs are equal.

B. Selection of the VRRM dimensions

The thickness of the stator yoke C is given by

$$C = \frac{D\beta_s}{2} \quad (9)$$

where β_s is the angle of stator polar arcs. The external

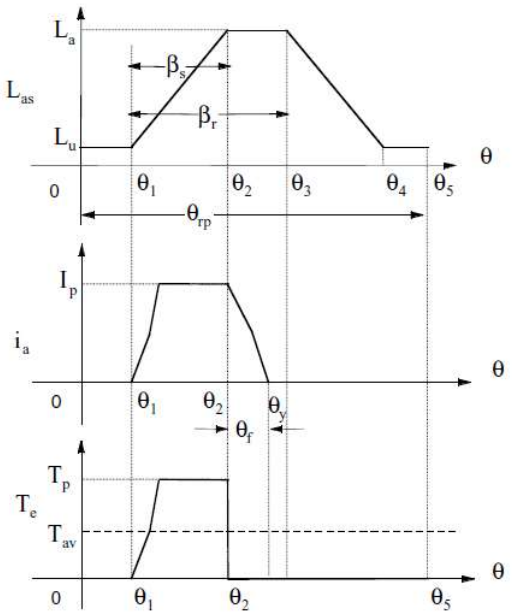

Fig. 2. Effect of rotor polar arc larger than the stator polar arc stator in the production of torque [8].

diameter D_0 is 1.4 to 2.5 times larger than the inner diameter. The stator pole height is, then, computed by

$$h_s = \frac{D_0}{2} - \frac{D}{2} - C \tag{10}$$

The width of the rotor yoke C_{ry} is

$$C_{ry} = \frac{D\beta_r}{2} \tag{11}$$

while the rotor pole height is given by

$$h_r = \frac{D}{2} - g - C_{ry} \tag{12}$$

The number of turns per phase T_{ph} is calculated by maximum rated current permitted by the machine, i, length, g, and the magnetic field strength in the air gap H_g

$$T_{ph} = \frac{2H_g g}{i} \tag{13}$$

$$H_g = \frac{B_g}{\mu_0} \tag{14}$$

For the dimensioning of the coil, the area and diameter of conductor, a_c and d_c, are respectively given by

$$a_c = \frac{i}{(J\sqrt{m})} \tag{15}$$

$$d_c = \sqrt{\frac{4a_c}{\pi}} \tag{16}$$

where J is the maximum current density allowed in the coil and m is the number of phases.

C. Converting rotary to linear parameters

The active stator fixed structure and passive moveable translator, the stator and the rotor of the VRRM initial design, corresponds respectively to the stator (active) and translator (passive) of LVRM considered in this case. Thus, the LVRM stator contains 8 poles, T_{sp}, and the translator has 6 poles, T_{tp}. The widths of the pole and the stator yoke, w_{ss} and w_{sp}, are respectively

$$w_{sp} = C \tag{17}$$

$$w_{ss} = \frac{\pi D - T_{sp} w_{sp}}{T_{sp}} \tag{18}$$

The widths of the pole and the yoke of translator, w_{tp} and w_{ts} respectively, they are

$$w_{tp} = C_{ry} \tag{19}$$

$$w_{ts} = \frac{\pi D - T_{tp} w_{tp}}{T_{tp}} \tag{20}$$

Therefore, the length of the stator is given by

$$L_{sr} = T_{sp} w_{sp} + (T_{sp} - 1) w_{ss} \tag{21}$$

The width of LVRM stack is equivalent to RVRM, so

$$L_w = L \tag{22}$$

The number of coil layers vertically and horizontally, N_v and N_h respectively, are given by

$$N_v = \frac{F_f (h_s - w)}{d_c} \tag{23}$$

$$N_h = T_{ph}(2N_v) \tag{24}$$

where F_f is the fill factor of the coil and w is the distance between the height of the pole and the height of the coil, called wedge. The area of the coil is then obtained by

$$Area = \frac{2\, ac\, N_v\, N_h}{F_f} \tag{25}$$

And the fill factor is given by

$$F_f = \frac{Area}{w_{ss}(h_s - w)} \tag{26}$$

The range of F_f values so that the coils do not touch one another is $0.2 < F_f < 0.5$.

D. Model dimensions

The LVRM is designed so that the translator has a five (5) meter length, L_t; the translator reaches a maximum speed (v_m) of 0.357 m/s and has an acceleration and deceleration time, t_a and t_d, both respectively equal to 1 second; and the translator mass M, is restricted to 274 kg. The maximum acceleration force, F_a produced by the active parte (the

stator) is given by the following equation

$$F_a = M * a_a \quad (27)$$

where a_a is the maximum acceleration of translator given by

$$a_a = \frac{v_m}{t_a} \quad (28)$$

For the VRRM design, the minimum stator polar arc is given by (7) $min(\beta_s) = 15^o$. Therefore, it is assumed that the polar arc is equal to $\beta_s = 16^o$. From (8), the rotor polar arc (translator) is set to $\beta_r = 20^o$. The following constants where selected (2)-(5) as follows: $k_e = 0.35$. $k_d = 1$, $k_2 = 0.72$, $k = 0.5$, $B_g = 0.98$ T, $A_{sp} = 41576.84$. B_g and A_{sp} are chosen by trial and error so that the flux density in the translator has its value at the "knee" point of the magnetization curve; and the acceleration force match with the simulated propulsion force through the finite element method (FEM). Equations from (1) to (28) are used in the initial calculations of the LVRM design. Table I shows the calculated dimensions and materials chosen. The magnetization curve for the magnetic material used is shown in Figure 3.

Table I
DIMENSIONS OF LVRM

Dimensions of LVRM (mm)				Characteristics of LVRM	
Width of LVRM	45	Height of translator pole	14	Number of turns per phase	221
Length of translator	322	Width of stator pole	20	Phase current	10A
Thickness of stator yoke	20	Width of stator slot	20	Maximum current density	5A/mm^2
Thickness of translator yoke	22	Width of translator pole	22	Wire	18 AWG
Height of stator pole	28	Width of translator slot	38	Magnetic material	Steel M-19
Air gap width	1	-	-	Phase number	4

3. Finite Elements Analysis

The use of Finite Element Method (FEM) simplifies solving problems, dividing the solution domain into several sub-areas (i.e. triangles) in order to bring the solutions of the magnetic vector potential A to a more precise solution [12]. The finite element analysis involves four steps[13]:

- Discretization of the solution region in a finite number of elements;
- Equations governing the problem for a typical element;
- Assembly of all the elements in the solution region;
- Solution of equations system obtained.
- The application of FEM is divided into three stages: preprocessing, processing and post-processing.

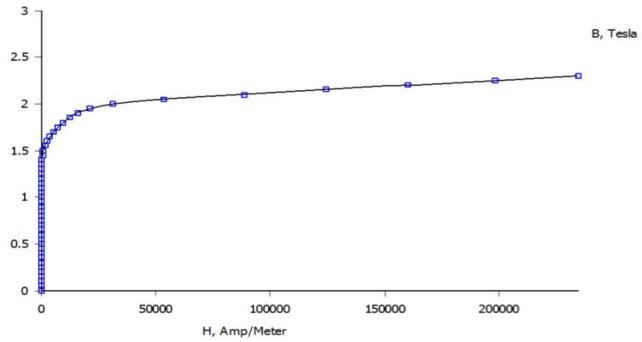

Figure 3. B-H magnetization curve of non-oriented-grain silicon steel (M-19 Steel).

A. Magnetostatic modeling

Electromagnetic phenomena are described by Maxwell equations, which constitute a system of partial differential equations. The equations governing the magnetostatic model are [12],

$$rot\ \vec{H} = \vec{J} \quad (29)$$

$$div\ \vec{B} = 0 \quad (30)$$

where $\vec{H}$ is the magnetic field intensity, $\vec{B}$ is the magnetic field density and $\vec{J}$ is the electric current density. For the modeling to be complete constitutive relations and boundary conditions must be met.

The LVRM design through the output power equation is verified through the inductance characteristics and normal and propulsion forces dependent of the translator position. Figs. 4 and 5 show the sketch of LVRM and flux lines in the 2D FEM software in the aligned and misaligned positions, respectively.

Both normal and propulsion forces are obtained through the integral block Weighted Stress Tensor. Fig. 6 present the values of inductance relatively to the translator position for the 10 A rated current. Fig. 7 presents the values of normal force obtained through the FEMM program. Figure 8 present the values of propulsion force relatively to the translator position.

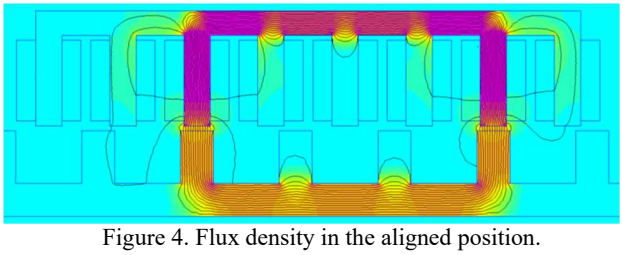
Figure 4. Flux density in the aligned position.

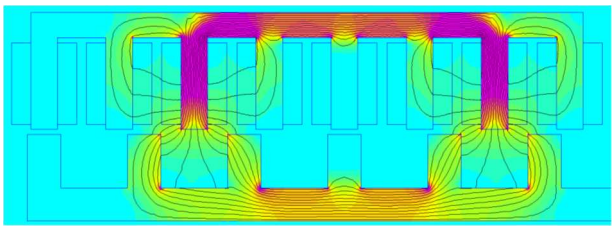

Figure 5. Flux density in the misaligned position.

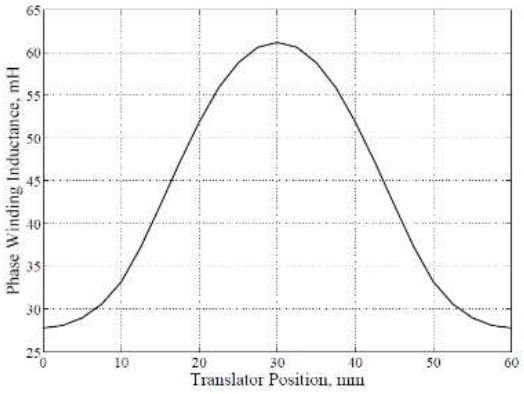

Figure 6. Inductance curve relatively to the translator position.

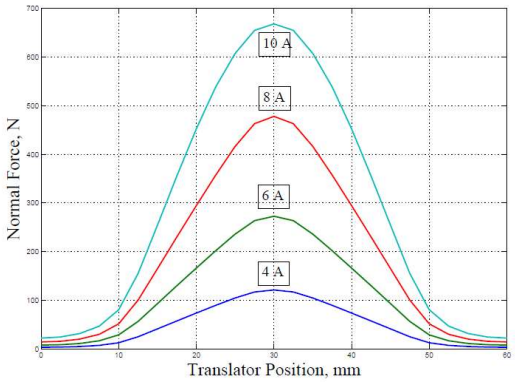

Figure 7. Normal force curve relatively to the translator position.

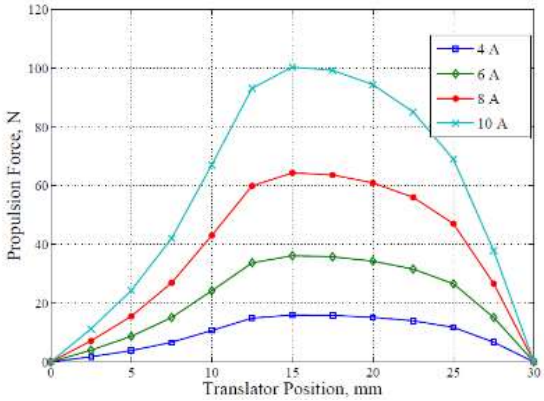

Figure 8. Propulsion force curve relatively to the translator position.

B. *Ratio of Pole Arc to Pole Pitch*

The pole pitch is the angle, or linear dimensions' length formed between two consecutive poles. The ration between the polar arcs and polar steps, defined as pole enclosure, is an important variable in LVRM design. The pole pitch in radians is given by

$$\theta_{rp} = \frac{2\pi}{P_r} \tag{31}$$

and the ratio is given by

$$\frac{\beta_r}{\theta_{rp}} = \frac{\beta_r P_r}{2\pi} \tag{32}$$

The analysis of the effects of variation of the polar arc is made in a way of that pole enclosure ratio keep constant. Note that the ratio (8) must be maintained in order to avoid producing negative torque, which reduces the ripple factor and hence the generation of noise [8]. Fig.9 shows the variation of thrust force as a function of the ratio of the polar arc and the pole pitch of the rotor pole enclosure.
The current configuration has a pole enclosure of 0.33. Indeed, it is one of the best possible configurations taking into consideration the propulsion force and the amount of magnetic material necessary for the construction of the motor.

C. *Force ripple*

The ripple factor can be determined from the variations of the propulsion force. Fig. 10 shows the maximum and minimum forces through two consecutive phases. Assuming that the maximum static force F_{max} and the minimum value that occurs in two intersection points of two consecutive phases as F_{min} [7], the percentage of ripple factor can be defined as

$$ripple(\%) = \frac{(F_{max} - F_{min})}{F_{avg}}.100 \tag{33}$$

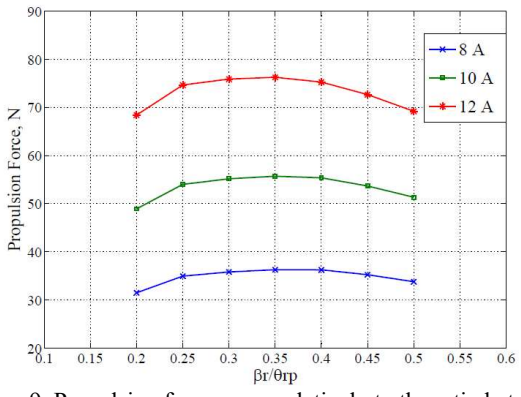

Figure 9. Propulsion force curve relatively to the ratio between translator polar arc and the pole step.

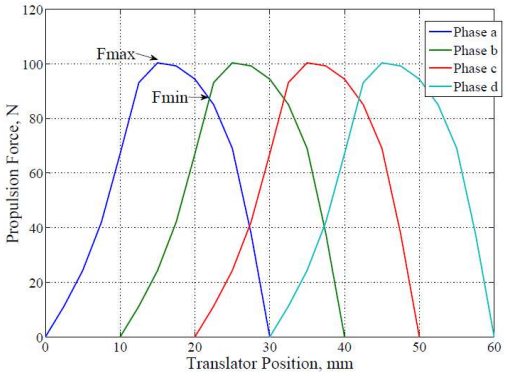

Figure 10. Propulsion force curve relatively to the translator position showing maximum and minimum forces.

Through (33), the percentage of ripple factor is approximately 15%, which indicates a good value for the LVRM given configuration. There is a proposal for minimization of ripple force using "pole shoes" [14]. However, it is a technique which makes the machine construction more difficult and adds good margin for reducing the ripple force.

4. Conclusions

The model designed for verification through FEMM is based in the output equation similar to the conventional ac machines. The results obtained were analyzed since the misalignment of poles until the complete alignment of poles of the machine. Inductance profiles, the normal and propulsion forces are compatible with the initial parameters of LVRM design. The acceleration force calculated by (27) required to translator movement is 97 N. Therefore, the value of the force obtained through the simulation was approximately 100 N, applying a rated current of 10 A, indicating that machine dimensions are appropriate to the suggested application.

As for the ripple factor, the four phases motor presented generates a percentage of about 15%, which is a good result compared to the three-phases LVRM's, generating a percentage of around 50% to 60%. The ratio of polar arches and polar pole steps is good, provided for the stator and translator, the values are 0.33 and 0.35, respectively. This result shows that the motor produces enough propulsion force to drive the load, maximizing efficiency with respect to use of resources or materials needed to manufacture the motor. Hysteresis effects and optimization of the dimensions of LVRM can be analyzed in future studies in order to improve the cost/benefit ratio of the machine.

Acknowledgements

The authors wish to thank the Coordination for the Improvement of Higher Education Personnel Agency (CAPES) of the Brazilian Ministry of Education for the financial resources for the development of this research work.

References

[1] H. S. Lim, R. Krishnan, N. S. Lobo, "*Design and Control of a Linear Propulsion System for an Elevator Using Linear Switched Reluctance Motor Drives"*, IEEE Transactions On Industrial Electronics, vol. 55, no. 2, February 2008.

[2] W. C. Gan, N. C. Cheung, and L. Qiu, *"Position control of linear switched reluctance motors for high-precision applications,"* IEEE Trans. Ind. Appl., vol. 39, no. 5, pp. 1350–1362, Sep./Oct. 2003.

[3] M. Dursun, F. Koc, H. Ozbay, S. Ozden, "*Design of Linear Switched Reluctance Motor Driver for Automatic Door Application"*, International Journal of Information and Electronics Engineering, Vol. 3, No. 3, May 2013.

[4] S. Muhammad, *"Analysis, Design and Control Aspects of Linear Machines Using Co-simulation,"* KTH Royal Institute of Technology, Sweden, 2012.

[5] H. Lee, K. Kim, J. Lee *"Review of Maglev Train Technologies,"* IEEE Transactions on Magnetics, vol. 42, no. 7, July 2006, pp. 1917-1926.

[6] R. Krishnan, R. Arumugam, J. F. Lindsay, *"Design Procedure for Switched-Reluctance Motors,"* IEEE Transactions on Industry Applications, vol. 24, no. 3, May/June, 1988, pp. 456-461.

[7] N. C. Lenin, R. Arumugam, *"Design and Experimental Verification of Linear Switched Reluctance Motor with Skewed Poles,"* International Journal of Power Electronics and Drive System, Vol. 6, No. 1, March 2015, pp. 18-25.

[8] R. Krishnan, *"Switched Reluctance Motor Drives Modeling Simulation Analysis Design and Applications,"* Industrial Electronics Series. CRC Press LLC, 1. ed, 2001, pp. 111-195.

[9] C. Praveen Kumar, K. Geetha, K. Madhavi, *"Design, Modeling and Analysis of Linear Switched Reluctance Motor for Ground Transit Applications,"* IOSR Journal of Electrical and Electronics Engineering (IOSR- JEEE). e-ISSN: 2278-1676,p-ISSN: 2320-3331, Volume 10, Issue 1 Ver. III (Jan – Feb. 2015), pp. 01-10.

[10] Byeong-Seok Lee, Han-Kyung Bae, V. Praveen, R. Krishnan, *"Design of a Linear Switched Reluctance Machine,"* IEEE Transactions On Industry Applications, Vol. 36, No. 6, November/December, 2000.

[11] Mr. Myo Min Thet, *"Design and Calculation of 75W Three-Phase Linear Switched Reluctance Motor,"* Department of Electrical Power Engineering, Mandalay Technological University, Myanmar, World Academy of Science, Engineering and Technology 48, 2008.

[12] D. Meeker *"Finite Element Method Magnetics,"* User's Manual, version 4.2, October 25, 2015.

[13] M. N. O Sadiku *"Numerical Techniques in Electromagnetics,"* CRC Press LLC, 2. ed, 2001.

[14] N. C Lenin, R. Arumugam, *"A Novel Linear Switched Reluctance Machine: Analysis and Experimental Verification",* Department of Electrical Engineering, St. Joseph's College of Engineering, Chennai, India, American J. of Engineering and Applied Sciences, ISSN 1941-7020, 2010.